

Published in final edited form as:

FEBS Lett. 2012 December 14; 586(24): . doi:10.1016/j.febslet.2012.10.044.

## Effects of the loss of the axial tyrosine ligand of the low-spin heme of MauG on its physical properties and reactivity

Nafez Abu Tarboush<sup>1</sup>, Sooim Shin<sup>2</sup>, Jiafeng Geng<sup>3</sup>, Aimin Liu<sup>3</sup>, and Victor L. Davidson<sup>2,‡</sup>

<sup>1</sup>Biochemistry and Physiology Department, College of Medicine, The University of Jordan, Amman, Jordan 11942

<sup>2</sup>Burnett School of Biomedical Sciences, College of Medicine, University of Central Florida, Orlando, FL 32827

<sup>3</sup>Department of Chemistry and Center for Diagnostics and Therapeutics, Georgia State University, Atlanta, GA, 30303

### Abstract

MauG catalyzes posttranslational modifications of methylamine dehydrogenase to complete the biosynthesis of its protein-derived tryptophan tryptophylquinone (TTQ) cofactor. MauG possesses a five-coordinate high-spin and a six-coordinate low-spin ferric heme, the latter with His-Tyr ligation. Replacement of this tyrosine with lysine generates a MauG variant with only high-spin ferric heme and altered spectroscopic and redox properties. Y294K MauG cannot stabilize the *bis*-Fe(IV) redox state required for TTQ biosynthesis but instead forms a compound I-like species on reaction with peroxide. The results clarify the role of Tyr ligation of the five-coordinate heme in determining the physical and redox properties and reactivity of MauG.

### 1. Introduction

MauG from *Paracoccus denitrificans* [1] is a diheme enzyme which catalyzes the biosynthesis of the protein-derived tryptophan tryptophylquinone (TTQ) cofactor [2] of methylamine dehydrogenase (MADH) [3]. The substrate for MauG is an MADH precursor protein (preMADH) in which residue  $\beta$ Trp57 has been monohydroxylated [4]. MauG catalyzes the six-electron oxidation of preMADH which results in crosslinking of  $\beta$ Trp57 and  $\beta$ Trp108, a second hydroxylation of  $\beta$ Trp57, and oxidation of the quinol species to the quinone [5,6] (Figure 1). Diferric MauG contains two *c*-type hemes. One is high-spin with His35 providing an axial ligand and the other is low-spin with axial ligands provided by His205 and Tyr294 [1,7]. Natural Tyr-His heme *c* ligation has not previously been described, and MauG is the first example of a *c*-type heme with axial ligation by tyrosine. Despite a 21 Å separation of the heme irons [7], the diheme system of MauG exhibits redox cooperativity with the two hemes behaving as a single diheme unit rather than as independent hemes [8]. As such, the two oxidation/reduction midpoint potential ( $E_m$ ) values for the inter-conversion between diferric and diferrous states correspond to the sequential addition or removal of the first and second electrons from the diheme system; rather than

© 2012 Federation of European Biochemical Societies. Published by Elsevier B.V. All rights reserved.

<sup>‡</sup>Address correspondence to: Burnett School of Biomedical Sciences, College of Medicine, University of Central Florida, 6900 Lake Nona Blvd., Orlando, FL 32827 Tel: 407-266-7111. Fax: 407-266-7002. victor.davidson@ucf.edu.

**Publisher's Disclaimer:** This is a PDF file of an unedited manuscript that has been accepted for publication. As a service to our customers we are providing this early version of the manuscript. The manuscript will undergo copyediting, typesetting, and review of the resulting proof before it is published in its final citable form. Please note that during the production process errors may be discovered which could affect the content, and all legal disclaimers that apply to the journal pertain.

being attributable to one or the other heme. A novel feature of MauG is that on reaction with H<sub>2</sub>O<sub>2</sub> it generates a *bis*-Fe(IV) state with the five-coordinate heme as Fe(IV)=O and the other heme as Fe(IV) with the two axial ligands from the protein retained [9]. This *bis*-Fe(IV) state is required for each of the three sequential two-electron oxidations of preMADH. The catalytic mechanism requires long range electron/hole transfer as the substrate is ~40 Å away from the oxygen-binding heme iron [7,10,11]. This mechanism also requires that solvent rather than the ferryl heme is the source of the oxygen that is added to β Trp57 during biosynthesis (Figure 1).

Previously Try294, the distal axial ligand of the low-spin heme, was mutated to His and the crystal structure of Y294H MauG revealed that the six-coordinate heme had His-His axial ligation [12]. Y294H MauG was able to interact with preMADH and participate in inter-protein electron transfer, but it was unable to catalyze the TTQ biosynthesis reactions that require the *bis*-Fe(IV) state. Spectroscopic data revealed that Y294H MauG could not stabilize the *bis*-Fe(IV) state, but instead formed a compound I-like species which could not catalyze TTQ biosynthesis [12].

In this study Tyr294 was converted to Lys, which resulted in loss rather than replacement of the axial heme ligand provided by Tyr294. This provides an opportunity to characterize a form of MauG with two five-coordinate hemes. The results of this study and previous work allow us to clarify the role of this novel Tyr ligation in determining the physical and redox properties and reactivity of MauG.

## 2. Materials and Methods

### 2.1. Protein Expression and Purification

Methods for the expression and purification of MADH [13], preMADH [4], and MauG [1] were as described previously. Site-directed mutagenesis to create Y294K MauG was performed on pMEG391 [1], which contains *mauG*, with the Quick-Change kit (Stratagene). The entire *mauG*-containing fragment was sequenced to ensure that no additional site mutations were present. Y294K MauG was expressed in *P. denitrificans* and isolated from the periplasmic fraction as described for recombinant wild-type (WT) MauG [1]. The yield was approximately 1 mg/L of culture, which is comparable to the yield of WT MauG.

### 2.2. EPR Spectroscopy

EPR samples were prepared in 50 mM potassium phosphate buffer, pH 7.4, with 150 μM WT or Y294K MauG. Continuous wave X-band EPR spectra were taken on a Bruker ER200D spectrometer at 100-kHz modulation frequency coupled with a dual mode resonator. The measurement temperature was maintained at 10 K with an ESR910 liquid helium cryostat and an ITC503 temperature controller from Oxford Instrument.

### 2.3. Redox Titrations

$E_m$  values were determined by anaerobic spectrochemical titration as described previously for WT MauG [8] using FMN as a mediator. Sodium dithionite and potassium ferricyanide were used in reductive and oxidative titrations, respectively. The titrations were fully reversible. The fraction reduced (eq 1) was determined by comparison with the spectra of the completely oxidized and reduced forms of MauG and quantitated from the absorbance at 550 nm, where  $a$  and  $(1 - a)$  are the fraction of the total absorbance change attributable to each of the two one-electron redox couples.  $E_m$  values are reported versus NHE.

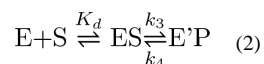
$$\text{Fraction reduced} = a / \left[ 1 + 10^{((E - E_{m1})/0.059V)} \right] + (1 - a) / \left[ 1 + 10^{(E - E_{m2})/0.059V} \right] \quad (1)$$

## 2.4. MauG-dependent TTQ Biosynthesis

Steady-state kinetic studies of MauG-dependent TTQ biosynthesis from preMADH were performed using a previously described spectrophotometric assay [14,15]. Y294K MauG was mixed with preMADH in 0.01 M potassium phosphate buffer, pH 7.5 at 25 °C. Reactions were initiated by addition of 100  $\mu$ M H<sub>2</sub>O<sub>2</sub> and the rate of appearance of quinone MADH was monitored at 440 nm.

## 2.5. Electron Transfer from Diferrous Y294K MauG to Quinone MADH

The single-turnover kinetics of the reaction of diferrous Y294K MauG with quinone MADH were studied as described previously for WT MauG [16]. The reaction was monitored by the decrease in absorbance at 550 nm which corresponds to the conversion of diferrous to diferric MauG [1]. Data were analyzed using equations 2 and 3 where S is quinone MADH, E is diferrous MauG, E' is diferric MauG, and P is quinol MADH.



$$K_{obs} = k_3 [S] / ([S] + K_d) + k_4 \quad (3)$$

## 3. Results

### 3.1. Effects of the Y294K Mutation on the Visible Absorption Spectra of Diferric and Diferrous MauG

It should be noted that since MauG is a diheme protein, its spectral features contributions from each heme. It was confirmed that Y294K MauG possessed two covalently bound hemes and the extinction coefficients of peaks in the absorption spectrum were determined by the pyridine hemochrome method [17]. Anaerobic titration of Y294K MauG with dithionite confirmed that two electron equivalents are required for conversion of the diferric to the diferrous state. The spectra of the diferrous and diferric forms reveal that the Y294K mutation caused subtle changes in the absorption maxima of the Soret and  $\beta$  peaks of MauG, as well as increases in the extinction coefficients for all peaks in the diferrous spectrum (Table 1). These changes are similar to spectral changes which were caused by the Y294H mutation of MauG [12].

### 3.2. Effects of the Y294K mutation on the EPR spectrum of MauG

Figure 2 presents the EPR spectra of WT and Y294K MauG. The Y294K EPR spectrum is dominated by high-spin heme signal ( $g = 5.57, 1.99$ ), which indicates that the hemes are primarily five-coordinate with axial His ligation. A minor low-spin ferric component with  $g$  values of 2.89, 2.32 and 1.52 is also apparent in the Y294K spectrum. This signal was previously seen in the spectrum of WT MauG and assigned as a six-coordinate artifact derived from the original five-coordinate heme after binding another ligand from solvent on freezing [15,18]. Mössbauer spectroscopy analysis of diferric WT MauG revealed that about half of the five-coordinate heme is converted to this six-coordinate artifact [18]. The conversion of high-spin to low-spin heme on freezing has been documented in other diheme enzymes [19-21]. Further evidence supporting this interpretation is that for a P107S mutation of MauG, which introduced a sixth ligand from protein to the high-spin heme, the freezing artifact was absent [15]. Thus, this spectral feature does not describe the true low-spin heme. The major low-spin ferric species ( $g = 2.54, 2.19, 1.87$ ) in the EPR spectrum of WT MauG, which corresponds to the six-coordinate His-Tyr ligated heme, disappears in the spectrum of Y294K MauG, consistent with loss of the Tyr heme ligand.

### 3.3. Effect of the Y294K Mutation on the $E_m$ Values of MauG

MauG exhibits two  $E_m$  values which correspond to the sequential addition or removal of the first and second electron from the diheme system [8]. Y294K MauG exhibited  $E_m$  values of  $-75$  and  $-268$  mV, whereas the  $E_m$  values for WT MauG are  $-158$  and  $-246$  mV (Figure 3, Table 2). The spectrochemical titration was reversible and yielded the same  $E_m$  values in each direction. The effect of this mutation is qualitatively similar to what was observed in Y294H MauG [12], except that in the latter case the increase in separation of the  $E_m$  values was much greater with  $E_m$  values of  $-17$  and  $-377$  mV.

### 3.4. Effect of the Y294K Mutation on Reaction of MauG with $H_2O_2$

Reaction of diferric MauG with  $H_2O_2$  results in the formation of a *bis*-Fe(IV) species which is reactive towards preMADH [9]. The formation and decay of this high-valent species is accompanied by changes in the visible absorption spectrum of MauG [22]. Reaction of Y294K MauG with  $H_2O_2$  caused spectral changes which were different from those observed for WT MauG (Figure 4). Upon reaction of WT MauG with  $H_2O_2$  the Soret band displays a red-shift of both sides of the absorption envelope, a slight shift in  $\lambda_{max}$ , and a decrease in intensity at  $\lambda_{max}$ . Reaction of Y294K MauG with  $H_2O_2$  results in a red-shift for only the lower wavelength side of the Soret band to produce a sharper peak, with a similar decrease in intensity. This result is similar to what was observed for Y294H MauG [12]. For that variant it was shown that addition of  $H_2O_2$  also resulted in the appearance of broad absorption in the 600-700 nm range with a major peak centered at 655 nm. The appearance of such absorption peaks in the 600-700 nm region with an accompanying decrease in absorption intensity of the Soret band is characteristic of Compound I (i.e., Fe(IV)=O<sup>+</sup>) species [19,23-26]. The same absorption feature was observed after addition of  $H_2O_2$  to Y294K MauG (Figure 4C), suggesting that it also forms a Compound I-like high-valent species rather than *bis*-Fe(IV). This high-valent species of Y294K MauG formed within the dead-time of mixing in stopped-flow experiments (i.e.,  $k > 300$  s<sup>-1</sup>) and it spontaneously decayed to the diferric state with a half-life of about three minutes (Figure 4D). This is similar to what was observed with WT MauG where the *bis*-Fe(IV) state also forms within the dead-time of mixing and exhibits a similar rate of spontaneous decay [22].

### 3.5. Effect of the Y294K Mutation on MauG-catalyzed TTQ Biosynthesis

Whereas the *bis*-Fe(IV) of WT MauG spontaneously decays to the diferric state slowly over several minutes, addition of preMADH to *bis*-Fe(IV) WT MauG accelerates the return to the diferric with a rate constant of  $0.8$  s<sup>-1</sup> [22]. In contrast, addition of preMADH to the high-valent compound I-like Y294K MauG species did not increase the slow rate of spontaneous return to the diferric state. Furthermore, when tested in steady-state kinetic assay of TTQ biosynthesis from preMADH, Y294K MauG was inactive (Table 2); results similar to those previously reported for Y294H MauG [12].

### 3.6. Effect of the Y294K Mutation on Electron Transfer from Diferrous MauG to Quinone MADH

In addition to the TTQ biosynthetic oxidation reactions which require formation of the *bis*-Fe(IV) intermediate [9,16], a thermodynamically favorable electron transfer from diferrous MauG to quinone MADH may be monitored [16]. This reaction does not require formation of the *bis*-Fe(IV) state and has been used to distinguish whether mutations of MauG affect stabilization of the *bis*-Fe(IV) state, the capacity for long range electron transfer between the redox centers of the proteins, or neither or both [10,12]. Y294K MauG was active in this reaction and exhibited a rate constant and  $K_d$  value of  $0.16$  s<sup>-1</sup> and  $14.4$   $\mu$ M, respectively, compared to  $0.07$  s<sup>-1</sup> and  $10.1$   $\mu$ M for WT MauG (Figure 5, Table 2).

## 4. Discussion

MauG is distinct from other heme proteins in its function and physical properties. It catalyzes three successive, different oxidation reactions on amino acid residues of a substrate protein via long range electron/hole transfer [7,10,11]. These oxidation reactions proceed via a *bis*-Fe(IV) intermediate in which the six-coordinate heme stabilizes the Fe(IV) state without an exogenous ligand [9]. An unprecedented structural feature of MauG is the His-Tyr axial ligation of the six-coordinate *c*-type heme [7]. Replacement of this Tyr with His to generate a His-His ligated heme abolished TTQ biosynthesis and the ability to stabilize the *bis*-Fe(IV) state [12]. To further probe the role of the distal axial ligand of the six-coordinate heme of MauG, a Y294K variant was created. The EPR spectrum of diferric Y294K MauG is consistent with the loss of the Tyr294 ligand of the native six-coordinate low-spin heme, which results in an enzyme with two five-coordinate hemes.

The properties of Y294K MauG are more similar to those of Y294H MauG than to those of WT MauG. The changes in the two  $E_m$  values caused by the Y294K mutation are similar to those caused by the Y294H mutation in that one  $E_m$  value increased and the other decreased. However, the magnitude of the changes was much less in Y294K MauG (Table 2). The fact that His-Tyr ligated heme in WT MauG is in a low-spin state rather than high-spin suggests that Tyr294 coordinates to the heme iron as a tyrosinate [27]. X-ray absorption and computational studies confirm that the heme ligand in WT MauG is the deprotonated tyrosinate in all redox states [28]. Thus, it is reasonable that the loss of that ligand or its replacement with His increases the  $E_m$  value for the first electron reduction by +83 mV for Y294K MauG and +141 mV for Y294H MauG (Table 2). It is not obvious why the  $E_m$  value for the second electron reduction is instead decreased relative to WT MauG. The basis for this phenomenon requires further study.

The most significant feature shared by Y294H and Y294K MauG is the formation of a high-valent Compound I-like species rather than the *bis*-Fe(IV) species. This renders both variants incapable of TTQ biosynthesis, in contrast to WT MauG which forms the *bis*-Fe(IV) species. Like Y294H MauG, Y294K MauG is competent in electron transfer from diferric MauG to quinone MADH, a reaction which does not require formation of the *bis*-Fe(IV) species. Thus, the mutation has not affected binding between the proteins or the electron transfer pathway that connects the redox centers, but rather the ability of the second heme to stabilize Fe(IV). The similar effects of either replacing the Tyr294 distal heme ligand with His [12], or the total loss of that ligand as in Y294K MauG, indicate that the changes in spectral properties and inability to stabilize the *bis*-Fe(IV) state are attributable primarily to the absence of Tyr as a heme ligand and that its replacement with an alternative ligand cannot compensate for the loss of Tyr. Furthermore, even though this heme in Y294K MauG lacks a distal ligand, the heme iron is apparently not accessible to H<sub>2</sub>O<sub>2</sub>. This highlights the functional role of this heme in electron transport rather than in binding exogenous ligands.

## Acknowledgments

We thank Yu Tang for technical assistance. This work was supported by NIH grant GM-41574 (VLD), NSF Grant MCB-0843537 (AL), Georgia Cancer Coalition Distinguished Scholar Program (AL) and fellowship support from the Molecular Basis of Disease program of Georgia State University (JG).

## References

- [1]. Wang Y, Graichen ME, Liu A, Pearson AR, Wilmot CM, Davidson VL. MauG, a novel diheme protein required for tryptophan tryptophylquinone biogenesis. *Biochemistry*. 2003; 42:7318–25. [PubMed: 12809487]



- [2]. McIntire WS, Wemmer DE, Chistoserdov A, Lidstrom ME. A new cofactor in a prokaryotic enzyme: tryptophan tryptophylquinone as the redox prosthetic group in methylamine dehydrogenase. *Science*. 1991; 252:817–24. [PubMed: 2028257]
- [3]. Davidson VL. Pyrroloquinoline quinone (PQQ) from methanol dehydrogenase and tryptophan tryptophylquinone (TTQ) from methylamine dehydrogenase. *Adv. Protein Chem.* 2001; 58:95–140. [PubMed: 11665494]
- [4]. Pearson AR, et al. Further insights into quinone cofactor biogenesis: probing the role of mauG in methylamine dehydrogenase tryptophan tryptophylquinone formation. *Biochemistry*. 2004; 43:5494–502. [PubMed: 15122915]
- [5]. Wang Y, Li X, Jones LH, Pearson AR, Wilmot CM, Davidson VL. MauG-dependent in vitro biosynthesis of tryptophan tryptophylquinone in methylamine dehydrogenase. *J. Am. Chem. Soc.* 2005; 127:8258–9. [PubMed: 15941239]
- [6]. Li X, Jones LH, Pearson AR, Wilmot CM, Davidson VL. Mechanistic possibilities in MauG-dependent tryptophan tryptophylquinone biosynthesis. *Biochemistry*. 2006; 45:13276–83. [PubMed: 17073448]
- [7]. Jensen LM, Sanishvili R, Davidson VL, Wilmot CM. In crystallo posttranslational modification within a MauG/pre-methylamine dehydrogenase complex. *Science*. 2010; 327:1392–4. [PubMed: 20223990]
- [8]. Li X, Feng M, Wang Y, Tachikawa H, Davidson VL. Evidence for redox cooperativity between c-type hemes of MauG which is likely coupled to oxygen activation during tryptophan tryptophylquinone biosynthesis. *Biochemistry*. 2006; 45:821–8. [PubMed: 16411758]
- [9]. Li X, Fu R, Lee S, Krebs C, Davidson VL, Liu A. A catalytic di-heme bis-Fe(IV) intermediate, alternative to an Fe(IV)=O porphyrin radical. *Proc. Natl. Acad. Sci. U S A.* 2008; 105:8597–600. [PubMed: 18562294]
- [10]. Abu Tarboush N, Jensen LMR, Yukl ET, Geng J, Liu A, Wilmot CM, Davidson VL. Mutagenesis of tryptophan199 suggests that hopping is required for MauG-dependent tryptophan tryptophylquinone biosynthesis. *Proc. Natl. Acad. Sci. USA.* 2011; 108:16956–16961. [PubMed: 21969534]
- [11]. Choi M, Shin S, Davidson VL. Characterization of electron tunneling and hole hopping reactions between different forms of MauG and methylamine dehydrogenase within a natural protein complex. *Biochemistry*. 2012; 51:6942–9. [PubMed: 22897160]
- [12]. Abu Tarboush N, Jensen LM, Feng M, Tachikawa H, Wilmot CM, Davidson VL. Functional importance of tyrosine 294 and the catalytic selectivity for the bis-Fe(IV) state of MauG revealed by replacement of this axial heme ligand with histidine. *Biochemistry*. 2010; 49:9783–91. [PubMed: 20929212]
- [13]. Davidson VL. Methylamine dehydrogenases from methylotrophic bacteria. *Methods Enzymol.* 1990; 188:241–6. [PubMed: 2126329]
- [14]. Li X, Fu R, Liu A, Davidson VL. Kinetic and physical evidence that the diheme enzyme MauG tightly binds to a biosynthetic precursor of methylamine dehydrogenase with incompletely formed tryptophan tryptophylquinone. *Biochemistry*. 2008; 47:2908–12. [PubMed: 18220357]
- [15]. Feng M, Jensen LM, Yukl ET, Wei X, Liu A, Wilmot CM, Davidson VL. Proline 107 is a major determinant in maintaining the structure of the distal pocket and reactivity of the high-spin heme of MauG. *Biochemistry*. 2012; 51:1598–606. [PubMed: 22299652]
- [16]. Shin S, Abu Tarboush N, Davidson VL. Long range electron transfer reactions between hemes of MauG and different forms of tryptophan tryptophylquinone of methylamine dehydrogenase. *Biochemistry*. 2010; 49:5810–6. [PubMed: 20540536]
- [17]. Berry EA, Trumpower BL. Simultaneous determination of hemes *a*, *b*, and *c* from pyridine hemochrome spectra. *Anal. Biochem.* 1987; 161:1–15. [PubMed: 3578775]
- [18]. Chen Y, et al. Role of calcium in metalloenzymes: effects of calcium removal on the axial ligation geometry and magnetic properties of the catalytic diheme center in MauG. *Biochemistry*. 2012; 51:1586–97. [PubMed: 22320333]
- [19]. Arciero DM, Hooper AB. A di-heme cytochrome-c peroxidase from *Nitrosomonas europaea* catalytically active in both the oxidized and half-reduced states. *J. Biol. Chem.* 1994; 269:11878–11886. [PubMed: 8163487]

- [20]. Foote N, Peterson J, Gadsby PMA, Greenwood C, Thomson AJ. Redox-linked spin-state changes in the di-heme cytochrome c-551 peroxidase from *Pseudomonas aeruginosa*. *Biochemical Journal*. 1985; 230:227–237. [PubMed: 2996492]
- [21]. Fulop V, Watmouth NJ, Ferguson SJ. Structure and enzymology of two bacterial di-heme enzymes: cytochrome *cd*<sub>1</sub> nitrite reductase and cytochrome *c* peroxidase. *Adv. Inorg. Chem.* 2001; 51:163–204.
- [22]. Lee S, Shin S, Li X, Davidson VL. Kinetic mechanism for the initial steps in MauG-dependent tryptophan tryptophylquinone biosynthesis. *Biochemistry*. 2009; 48:2442–7. [PubMed: 19196017]
- [23]. Makris TM, von Koenig K, Schlichting I, Sligar SG. The status of high-valent metal oxo complexes in the P450 cytochromes. *J Inorg Biochem*. 2006; 100:507–18. [PubMed: 16510191]
- [24]. Sheng X, Horner JH, Newcomb M. Spectra and kinetic studies of the compound I derivative of cytochrome P450 119. *J Am Chem Soc*. 2008; 130:13310–20. [PubMed: 18788736]
- [25]. Dolphin D, Forman A, Borg DC, Fajer J, Felton RH. Compounds I of catalase and horse radish peroxidase: pi-cation radicals. *Proc Natl Acad Sci U S A*. 1971; 68:614–8. [PubMed: 5276770]
- [26]. Bell SR, Groves JT. A Highly Reactive P450 Model Compound I. *J. Am. Chem. Soc.* 2009; 131:9640–9641. [PubMed: 19552441]
- [27]. Das TK, Couture M, Lee HC, Peisach J, Rousseau DL, Wittenberg BA, Wittenberg JB, Guertin M. Identification of the ligands to the ferric heme of *Chlamydomonas* chloroplast hemoglobin: evidence for ligation of tyrosine-63 (B10) to the heme. *Biochemistry*. 1999; 38:15360–8. [PubMed: 10563822]
- [28]. Jensen LM, Meharena YT, Davidson VL, Poulos TL, Hedman B, Wilmot CM, Sarangi R. Geometric and electronic structures of the His-Fe(IV)=O and His-Fe(IV)-Tyr hemes of MauG. *J. Biol. Inorg. Chem.* 2012 in press.

### Highlights

A Y294K mutation results in loss rather than replacement of the axial heme ligand provided by Tyr294

A Y294K mutation alters spectroscopic and redox properties of both hemes of MauG

Y294K MauG forms a high valent compound I-like species rather than a *bis*-Fe(IV) species

Y294K MauG is competent in long range electron transfer but has lost TTQ biosynthesis activity



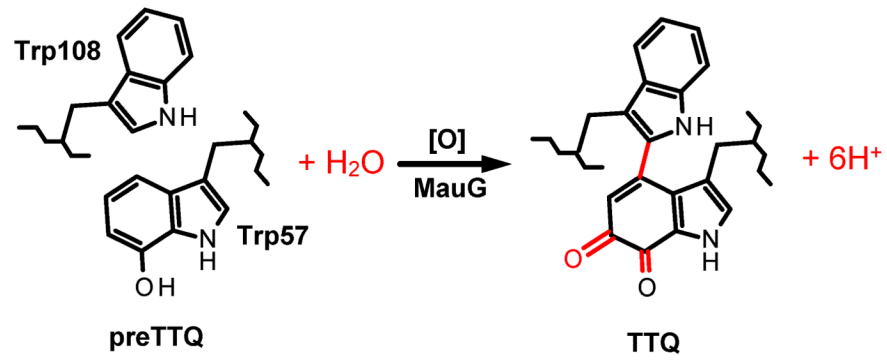


**Figure 1.**

MauG-dependent TTQ biosynthesis. Oxidation equivalents [O] may be provided by H<sub>2</sub>O<sub>2</sub> or O<sub>2</sub> plus a reductant. Posttranslational modifications which are catalyzed by MauG are shown in red.

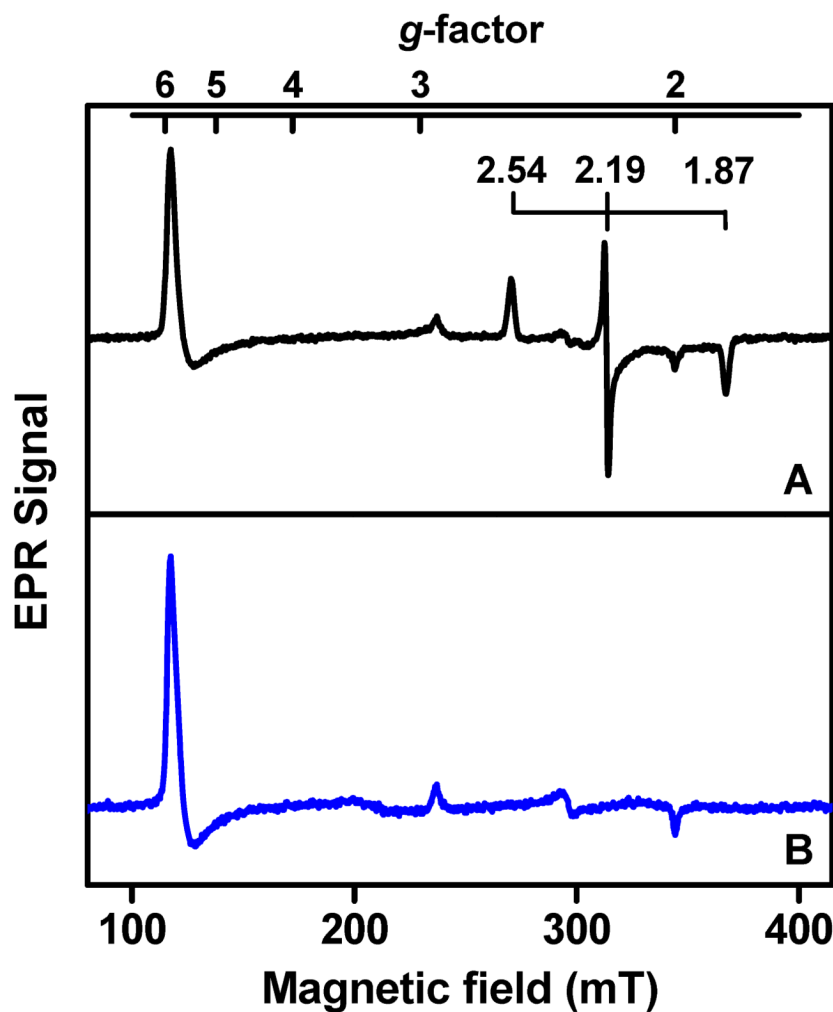


**Figure 2.** EPR spectra of WT (A) and Y294K (B) MauG. The low-spin ferric species in the spectrum of WT MauG, which corresponds to the His-Tyr ligated heme, is labeled for clarification. Samples containing 150  $\mu$ M WT or Y294K MauG were prepared in 50 mM potassium phosphate buffer, pH 7.4. Spectra were obtained at 10 K with microwave frequency, 9.65 GHz, microwave power, 1 mW, and modulation magnitude, 0.5 mT.

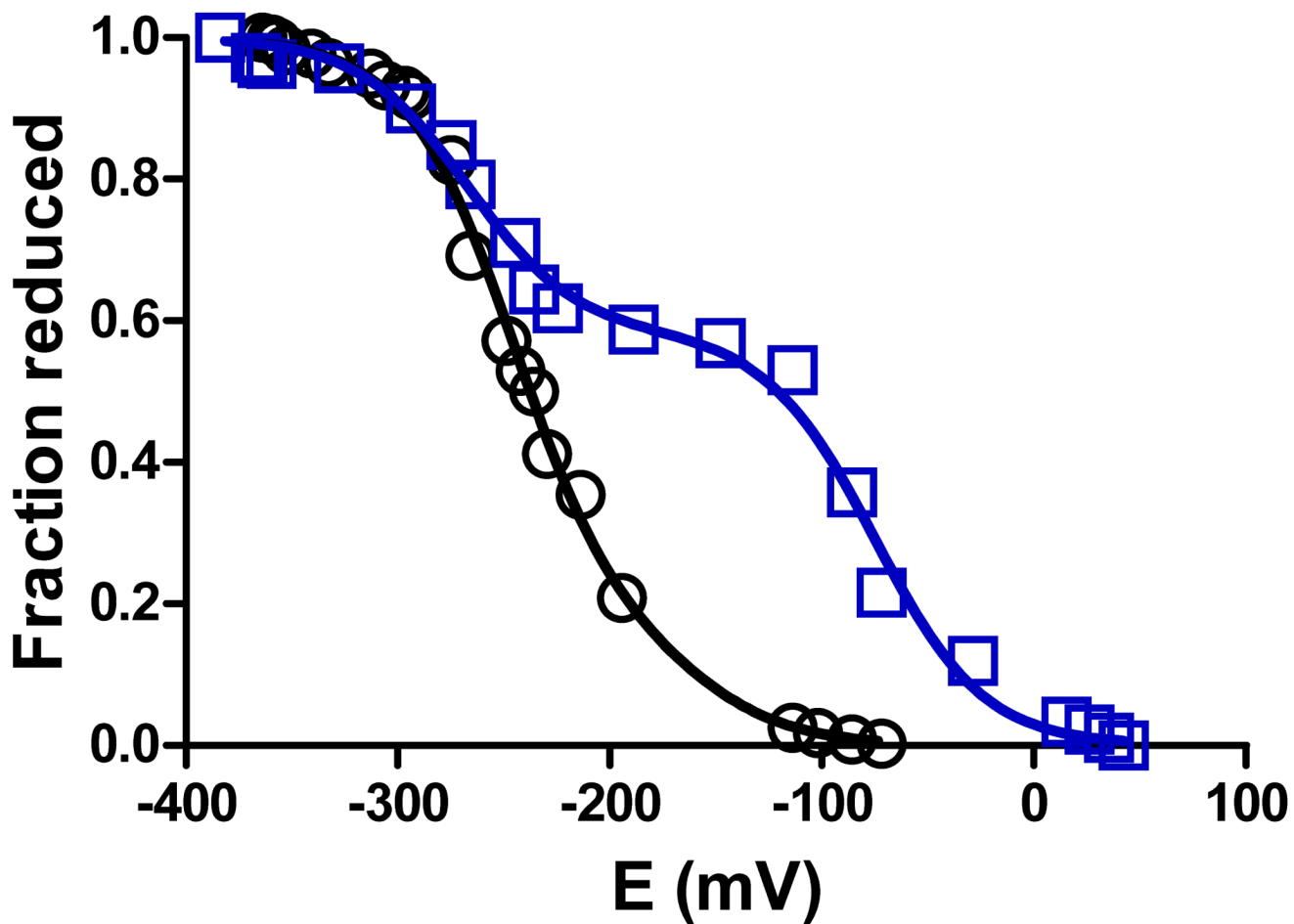


**Figure 3.** Spectrochemical redox titrations of WT MauG (circles, black) and Y294K MauG (squares, blue). Titrations were performed anaerobically in 50 mM potassium phosphate, pH 7.5, at 25 °C as described in section 2.3. Solid lines are fits of the data by eq 1.

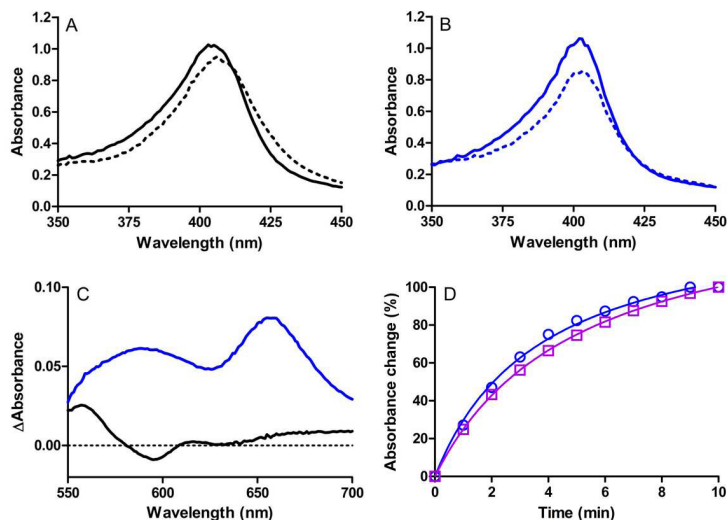


**Figure 4.**

Changes in the absorption spectra of WT and Y294K MauG upon addition of a stoichiometric amount of H<sub>2</sub>O<sub>2</sub>. (A) Soret region of 3 μM WT MauG before (solid line) and immediately after (dashed line) addition of H<sub>2</sub>O<sub>2</sub>. (B) Soret region of 3 μM Y294K MauG before (solid line) and immediately after (dashed line) addition of H<sub>2</sub>O<sub>2</sub>. (C) Difference spectra (immediately after addition of H<sub>2</sub>O<sub>2</sub> minus diferric spectra) of the higher wavelength region of the spectra for 15 μM WT MauG (black) or Y294K MauG (blue). (D). Time course for the return to the diferric state after addition of H<sub>2</sub>O<sub>2</sub> to generate the high-valent species in Y294K MauG. The changes in absorbance were monitored at 404 nm (blue circles) and 655 nm (purple squares). All spectra were recorded in 50 mM potassium phosphate, pH 7.5, at 25 °C.

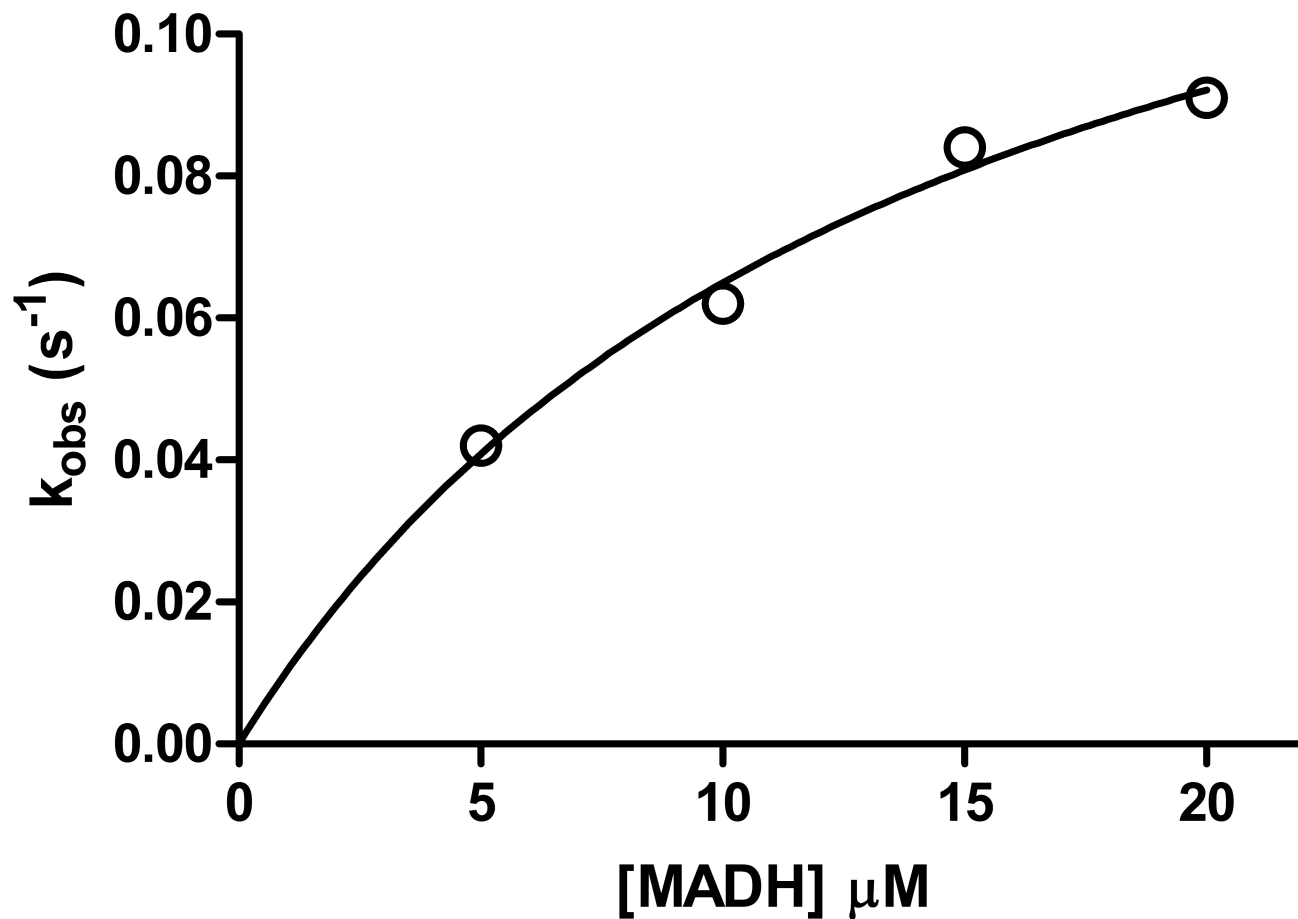


**Figure 5.** Single-turnover kinetics of the reaction of diferrous Y294K MauG. Each reaction was performed in 0.01 M potassium phosphate buffer, pH 7.5, at 25 °C. The reaction mixture contained 1.5  $\mu\text{M}$  of the limiting reactant, diferrous Y294K MauG. The line represents the fit of the data by eq 3.

**Table 1**

Effects of the Y294K mutation on absorption maxima ( $\lambda_{\max}$ ) and extinction coefficients ( $\epsilon$ ) of different redox forms of MauG.

Redox state	$\lambda_{\max}$ ( $\epsilon$ )nm ( $\text{mM}^{-1}\text{cm}^{-1}$ )		
	MauG	Y294K MauG	Y294H MauG <sup>a</sup>
Diferric	406 (309)	403 (348)	404 (347)
Diferrous	418 (327)	415 (411)	416 (434)
	524 (34)	522 (41)	522 (39)
	552 (50)	550 (61)	550 (66)
High valent	407 (271)	403 (280)	406 (286)
	-	655 (9.0)	655 (8.5)

<sup>a</sup>Values for Y294H MauG were taken from reference [12]



**Table 2**

Effects of the Y294K mutation on redox properties and reactivity of MauG.

Properties	WT MauG	Y294K MauG	Y294H MauG <sup>a</sup>
$E_m$ values (mV)	-158 ± 9 -246 ± 3	-75 ± 4 -268 ± 5	-17 ± 13 -377 ± 2
$k_{cat}$ for TTQ biosynthesis from preMADH (s <sup>-1</sup> )	0.2 <sup>b</sup>	0	0
$k_{cat}$ for TTQ biosynthesis from quinol MADH (s <sup>-1</sup> )	4.2 <sup>c</sup>	0	0
Electron transfer reaction from diferrous MauG to quinone MADH (s <sup>-1</sup> )	$k = 0.07 \pm 0.01 \text{ s}^{-1c}$ $K_d = 10.1 \pm 1.6 \mu\text{M}^c$	$k = 0.16 \pm 0.02 \text{ s}^{-1}$ $K_d = 14.4 \pm 3.4 \mu\text{M}$	$k = 0.21 \pm 0.01 \text{ s}^{-1}$ $K_d = 9.4 \pm 1.1 \mu\text{M}$

<sup>a</sup>Values for Y294H MauG were taken from reference [12]<sup>b</sup>Taken from reference [14]<sup>c</sup>Taken from reference [16]